Evidence for a Hard Ionizing Spectrum from a

The Astrophysical Journal Letters, 836:L14 (7pp), 2017 February 10 https://doi.org/10.3847/2041-8213/836/1/L14

Evidence for a Hard Ionizing Spectrum from a $z = 6.11$ Stellar Population

Ramesh Mainali[1], Juna A. Kollmeier[2], Daniel P. Stark[1], Robert A. Simcoe[3], Gregory Walth[4], Andrew B. Newman[2], and Daniel R. Miller[3]
[1] Department of Astronomy, Steward Observatory, University of Arizona, 933 North Cherry Avenue, Rm N204, Tucson, AZ, 85721, USA
rmainali@email.arizona.edu
[2] Carnegie Observatories, 813 Santa Barbara Street, Pasadena, CA 91101, USA
[3] MIT-Kavli Center for Astrophysics and Space Research, 77 Massachusetts Avenue, Cambridge, MA 02139, USA
[4] University of California, Center for Astrophysics and Space Sciences, 9500 Gilman Drive, San Diego, CA 92093, USA
Received 2016 November 22; revised 2017 January 13; accepted 2017 January 16; published 2017 February 10

Abstract

We present the *Magellan*/FIRE detection of highly ionized C IVλ1550 and O III]λ1666 in a deep infrared spectrum of the $z = 6.11$ gravitationally lensed low-mass galaxy RXC J2248.7-4431-ID3, which has previously known Lyα. No corresponding emission is detected at the expected location of He IIλ1640. The upper limit on He II, paired with detection of O III] and C IV, constrains possible ionization scenarios. Production of C IV and O III] requires ionizing photons of 2.5–3.5 Ryd, but once in that state their multiplet emission is powered by collisional excitation at lower energies ($\sim$0.5 Ryd). As a pure recombination line, He II emission is powered by 4 Ryd ionizing photons. The data therefore require a spectrum with significant power at 3.5 Ryd but a rapid drop toward 4.0 Ryd. This hard spectrum with a steep drop is characteristic of low-metallicity stellar populations, and less consistent with soft AGN excitation, which features more 4 Ryd photons and hence higher He II flux. The conclusions based on ratios of metal line detections to helium non-detection are strengthened if the gas metallicity is low. RXJ2248-ID3 adds to the growing handful of reionization-era galaxies with UV emission line ratios distinct from the general $z = 2$–3 population in a way that suggests hard ionizing spectra that do not necessarily originate in AGNs.

Key words: cosmology: observations – galaxies: evolution – galaxies: formation – galaxies: high-redshift

1. Introduction

Over the past year, the first detailed spectroscopic measurements constraining the nature of $z > 6$ star-forming galaxies have emerged (see Stark 2016 for a review), suggesting a different population than is common at $z \simeq 2$–3. Deep near-infrared spectroscopy has revealed strong UV metal line emission in galaxies at $z = 6$–8 with equivalent widths 5–10$\times$ larger than are typical at $z \simeq 2$ (Stark et al. 2015a, 2015b, 2017), while ALMA observations have begun to deliver detections of [C II] 158 μm and [O III] 88 μm emission in typical galaxies at $z > 6$ (Willott et al. 2015; Bradač et al. 2016; Inoue et al. 2016; Pentericci et al. 2016). Perhaps the most surprising result is the discovery of nebular C IV$\lambda\lambda$1548, 1550 in a galaxy at $z = 7.045$ (Stark et al. 2015b), requiring an extremely hard radiation field capable of producing a large number of photons more energetic than 47.9 eV. Only one percent of UV-selected galaxies at $z \simeq 3$ show strong nebular C IV emission (Steidel et al. 2002; Reddy et al. 2008; Hainline et al. 2011). While these systems tend to be low-luminosity narrow-line AGNs, more recent studies have shown that nebular C IV is also found in dwarf star-forming galaxies (Christensen et al. 2012; Stark et al. 2014; Vanzella et al. 2016), presumably powered by the harder radiation field from low-metallicity stars. The detection of nebular C IV in one of the first galaxies targeted in the reionization era suggests that galaxies with hard ionizing spectra may be more common in the reionization era.

There are two outstanding issues that must be addressed following these preliminary spectroscopic studies. First, it remains unclear how representative the $z = 7.045$ C IV emitter is of star-forming galaxies at $z > 7$. If stellar populations commonly produce hard ionizing spectra at $z > 6$, it would represent a rapid and qualitative change in the galaxy population relative to all lower redshifts, and these galaxies would play a larger role in reionization than has previously been assumed. Second, one must attempt to establish whether the high ionization emission is powered by hot, low-metallicity stars or AGNs. Both can potentially provide high-energy photons, and with a single metal line detection it is difficult to prove the source beyond a reasonable doubt (e.g., Stark et al. 2015b). At lower redshifts, the separation of AGNs and star-forming galaxies is readily carried out using rest-frame optical emission line ratios (e.g., Baldwin et al. 1981). However, utilization of a similar approach at $z > 6$ must await the launch of *JWST*. Recent efforts have begun to develop rest-UV diagnostics based on different photoionization models to distinguish the sources of ionizing spectra (Feltre et al. 2016). This can be achieved with current ground-based facilities, provided multiple far-UV lines can be detected.

In this paper, we describe the initial results from a spectroscopic campaign using the *Magellan* Baade Folded-port InfraRed Echellette (FIRE; Simcoe et al. 2013) aimed at addressing the two issues described above. The spectral coverage provided by FIRE makes it particularly efficient at recovering multiple lines in bright $z > 6$ galaxies. Here we describe FIRE observations of a $z = 6.110$ gravitationally lensed galaxy. The FIRE spectrum reveals the presence of the nebular C IVλ1550 emission line, providing another instance of high ionization lines at $z > 6$. We also report the detection of a second feature (O III]$\lambda\lambda$1660, 1666), enabling exploration of the origin of the high ionization emission.

Throughout the paper we adopt standard ΛCDM cosmology with $\Omega_M = 0.3$, $\Omega_\Lambda = 0.7$, $H_0 = 100\,h\,\mathrm{km\,s^{-1}\,Mpc^{-1}}$, and $h = 0.7$. Magnitudes are quoted in AB magnitudes.

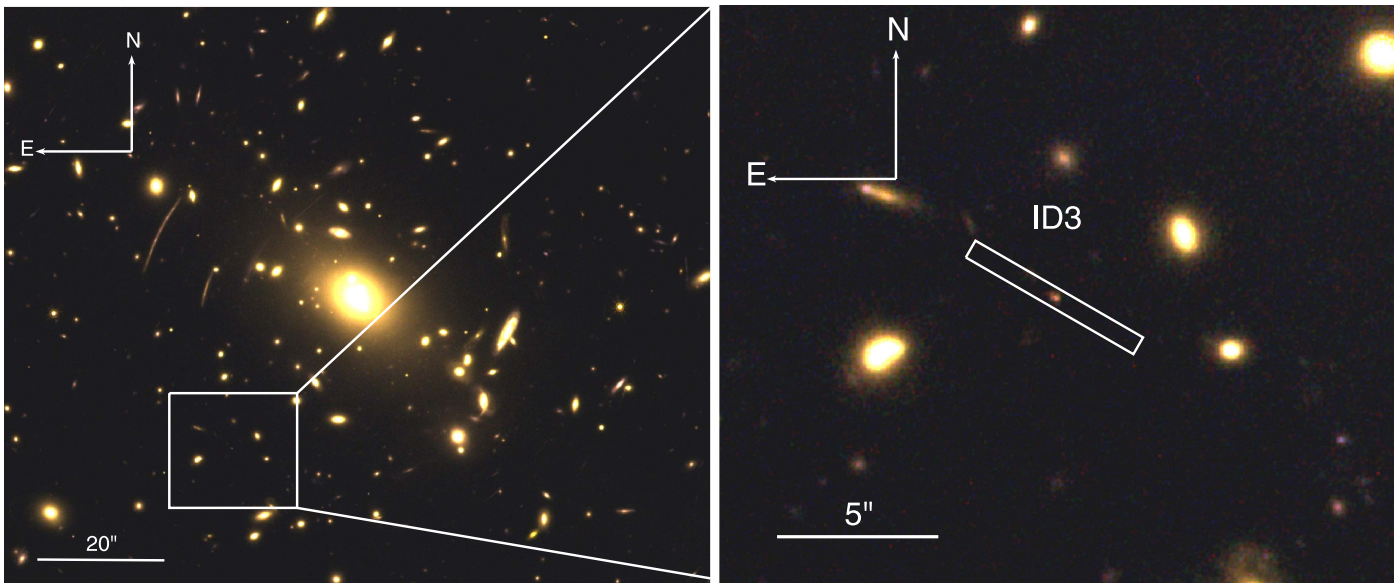

Figure 1. (Left) *HST* WFC3/IR color image of the cluster RXC J2248 showing the position of the galaxy RXC J2248-ID3. (Right) Slit center and position angle of the *Magellan*/FIRE observations.

2. Observations

We report on observations of RXC J2248-ID3, one of five images of a $z = 6.11$ gravitationally lensed galaxy behind the cluster RXC J2248.7-4431. The galaxy was first identified by Boone et al. (2013) and Monna et al. (2014) via the Cluster Lensing And Supernova survey with Hubble (Postman et al. 2012). The images are bright ($J_{125} = 24.8$–25.9), owing to their magnification (2.2–8.3×). We calculate the UV continuum slope using deeper imaging from the Hubble Frontier Field initiative (Lotz et al. 2014). The data show that the galaxy is very blue ($\beta = -2.54 \pm 0.16$) and that the UV absolute magnitude is $M_{\rm UV} = -20.1 \pm 0.2$ after magnification correction, indicating a sub-L* luminosity. As in our previous studies (i.e., Stark et al. 2013, 2017), we perform SED fitting using a code developed by Robertson et al. (2010) that combines the findings of Bruzual & Charlot (2003) with nebular line and continuum emission computed assuming case B recombination and empirical metallic line intensities from Anders & Fritze-v. Alvensleben (2003). For a Salpeter stellar IMF and constant star formation, the magnification-corrected data suggest a low stellar mass ($1 \times 10^8\ M_\odot$), little reddening ($E(B-V) = 0.01$), and a large sSFR (50 Gyr^{-1}). Strong Lyα ($W_{\rm Ly\alpha} = 75$ Å) has been identified in RXC J2248-ID3 by VLT/VIMOS (Balestra et al. 2013), VLT/FORS (Boone et al. 2013), and the *HST* WFC3/IR grism (Schmidt et al. 2016), consistent with expectations for young, metal-poor galaxies (e.g., Cowie et al. 2011; Trainor et al. 2016).

UV metal lines tend to be most prominent in systems with extremely large EW Lyα emission (e.g., Shapley et al. 2003; Stark et al. 2014), making RXC J2248-ID3 an ideal candidate for detecting metal lines at $z > 6$. At the redshift of RXC J2248-ID3, the FIRE spectrum is able to constrain the relative strengths of the Lyα, C IV$\lambda\lambda$1548, 1550, He IIλ1640, and O III] $\lambda\lambda$1660, 1666 lines. Unfortunately, the C III]$\lambda\lambda$1907, 1909 doublet is situated in a region of low atmospheric transmission between the J and H-bands, precluding useful flux constraints.

We observed RXC J2248-ID3 over 2014 July 19–21 using FIRE in echelle mode, providing continuous spectral coverage between 0.82 and 2.51 μm. The particular image we observed is magnified by 5.5×. We adopted a slit width of 0.″6, resulting in a resolving power of $R = 6000$. The orientation of the slit on the galaxy (PA = 60°) is shown in Figure 1. The exposures were carried out using two dither positions separated by 3.″0. Observing conditions were excellent, with clear sky and an average seeing of 0.″4. Given the seeing, source size, and slit width, we require a small aperture correction (1.1×) to the observed fluxes. The total on-source integration time over three nights was 9.17 hr.

The FIRE spectrum was reduced using standard routines in the FIREHOSE data reduction pipeline.[5] The pipeline uses lamp and sky flats. Two-dimensional sky models are iteratively calculated following Kelson (2003). The wavelength solutions are provided by fitting OH skylines in the spectra. Flux calibration and telluric corrections to the data are applied using A0V star observations. Finally, the 1D spectra were extracted using a boxcar with aperture of 1.″35 (15 pixels), corresponding to the spatial extent of the strongest emission line (Lyα) in the FIRE spectrum.

The *HST* grism spectra for RXC J2248 come from the GLASS survey (Grism Lens-Amplified Survey from Space; Schmidt et al. 2014; Treu et al. 2015). The *HST* WFC3/IR grisms G102 and G141 have a spectral resolution of 210 and 130 and cover the wavelengths 0.8–1.15 μm and 1.1–1.7 μm. The data were reduced using aXe (Kümmel et al. 2009). MultiDrizzle was used to combine the direct images. Multiple visits at similar roll angles were drizzled together and tweakshifts was used to determine the offset between the visits. Next, SExtractor was run on the direct images to generate the aXe input catalog. Finally, the aXe routines were run to drizzle the 2D spectra and extract the spectra. The 1D spectra were extracted from the 2D spectra using a 0.″38 (3 pixels) aperture. The extracted 1D spectra were then divided by the instrument sensitivity function and pixel size to flux-calibrate the spectra. The first roll angle (97.°7) had a significant contaminating continuum; a sliding median with a window of

[5] wikis.mit.edu/confluence/display/FIRE/FIRE+Data+Reduction

Table 1
Rest-UV Emission Line Measurements of the $z = 6.11$ Galaxy RXC J2248-ID3 from *Magellan*/FIRE and the *HST* WFC3/IR Grism

	λ_{rest}[a] (Å)	λ_{obs} (Å)	Line Flux (10^{-18} erg cm^{-2} s^{-1})	W_0 (Å)
Magellan/FIRE				
Lyα	1215.67	8643.5	33.2 ± 2.3	39.6 ± 5.1
N V	1240	…	<1.8	<2.3
C IV	1548.19	…	…	…
…	1550.77	11023.8	5.7 ± 0.9	9.9 ± 2.3
He II	1640.42	…	<1.5	<2.8
O III]	1660.81	11796.9	1.7 ± 0.6	2.9 ± 1.4
…	1666.15	11837.1	2.7 ± 0.6	4.6 ± 1.6
HST NIR WFC3 G102/G141				
C IV	1549[b]	…	14.0 ± 3.8	24.5 ± 7.1
O III]	1663[c]	…	<7.6	<13.0
C III]	1908[d]	…	<3.6	<7.9

Notes. Non-detections are listed as 2σ upper limits.
[a] Vacuum wavelengths.
[b] Total C IV$\lambda\lambda$1548, 1550 flux.
[c] Total O III]$\lambda\lambda$1660, 1666 flux.
[d] Total C III]$\lambda\lambda$1907, 1909 flux.

50 pixels (1200 Å) was used to subtract off the continuum source.

3. Results

We summarize line measurements in Table 1. Strong Lyα emission is clearly visible at 8643.5 Å in the FIRE spectrum (Figure 2(a)), implying a redshift ($z_{Ly\alpha} = 6.110$) that is consistent with the Lyα wavelength presented in Balestra et al. (2013). Using the redshift and spatial position defined by Lyα, we search for and characterize the strength of other emission lines in the FIRE spectrum. The nebular C IV $\lambda\lambda$1548, 1550 doublet is a resonant feature and is often scattered away from the line center. Observations of metal-poor star-forming galaxies with strong UV metal lines show that the peak C IV flux often has the same velocity offset from systemic as Lyα (Stark et al. 2015b; Vanzella et al. 2016). For a 10 Å window centered at the Lyα redshift, the C IVλ1548 line would be located at 11003 and 11013 Å and C IVλ1550 would lie between 11021 and 11031 Å. We clearly detect the C IVλ1550 component with S/N = 6.3 in the expected window at 11023.8 Å (Figure 2(b)). The line is barely resolved with a FWHM (corrected for instrumental resolution) of 59 km s^{-1}. The total integrated flux is $(5.7 \pm 0.9) \times 10^{-18}$ erg cm^{-2} s^{-1}. As is standard practice for faint high-redshift spectra lacking continuum detections, we compute the underlying continuum flux density at 1550 Å using the SED model that provides the best fit to the photometry (see Section 2 for details). This translates to a rest-frame equivalent width of 9.9 ± 2.3 Å, where the error includes the uncertainty in the continuum and line measurements. As is evident in Figure 2(b), a strong OH skyline is present at the expected location of C IVλ1548, precluding useful flux constraints for the blue component of the doublet. Observations of metal-poor C IV emitters often show equal flux in the two components of the doublet (e.g., Christensen et al. 2012; Stark et al. 2014). If this is also the case for RXC J2248-ID3, we would expect a total C IV line flux of 11.4×10^{-18} erg cm^{-2} s^{-1}. The theoretically expected flux ratio (C IVλ1548/C IVλ1550 = 2) has also been observed in several intermediate-redshift systems (e.g., Caminha et al. 2016; Vanzella et al. 2016) and would instead predict a total flux of 17.1×10^{-18} erg cm^{-2} s^{-1}.

Unlike the resonant C IV line, the nebular He IIλ1640 and O III] $\lambda\lambda$1660, 1666 lines typically trace the systemic redshift (Shapley et al. 2003; Steidel et al. 2010; Stark et al. 2014). Assuming Lyα velocity offsets ($\Delta v_{Ly\alpha}$) between 0 km s^{-1} and 450 km s^{-1}, consistent with previous studies (Tapken et al. 2007; Erb et al. 2010; Stark et al. 2015b, 2017), we predict that O III]λ1660 will fall between 11794 and 11808 Å and the O III]λ1666 will lie between 11832 and 11846 Å. We detect a 4.5σ emission feature (FWHM = 58 km s^{-1}) centered at 11837.1 Å (see Figure 2(d)) with total flux $(2.7 \pm 0.6) \times 10^{-18}$ erg cm^{-2} s^{-1}. We identify this line as O III]λ1666, indicating a systemic redshift of $z = 6.1045$ for RXC J2248-ID3. Following the same procedure described above for C IV, we calculate a rest-frame equivalent width of 4.6 ± 1.6 Å. Using the O III]λ1666 redshift, we search for emission associated with O III]λ1660. A faint emission component (S/N = 2.8) is visible at the expected wavelength (Figure 2(d)). The line flux and rest-frame equivalent width are $(1.7 \pm 0.6) \times 10^{-18}$ erg cm^{-2} s^{-1} and 2.9 ± 1.4 Å, respectively. Based on the presence of C IV, we may also expect to see nebular He II. While the line is expected to fall in a clean region of the FIRE spectrum at 11655 Å (based on the systemic redshift), there is no evidence of any emission feature at the expected location (Figure 2(c)), implying a 2σ upper limit on the rest-frame equivalent width of 2.8 Å. The non-detection of He II is consistent with the upper limits (<1.4 Å) derived for young metal-poor galaxies at $z \sim 2$–3 (e.g., Stark et al. 2014). Similarly, we do not detect the N V$\lambda\lambda$1238, 1240 line ($W_{N\,V} < 2.3$ Å) that is commonly seen in AGN spectra.

The systemic redshift provided by the detection of O III] allows Lyα to be shifted to the galaxy rest-frame. Figure 3(a) shows the resultant Lyα line profile. The peak Lyα flux is redshifted from systemic by a velocity offset of $\Delta v_{Ly\alpha} = 235$ km s^{-1}. The FWHM of the Lyα (131 km s^{-1}) is narrower than many luminous reionization-era galaxies with Lyα detections (e.g., Oesch et al. 2015). The difference with respect to the C IV and O III] FWHM is not surprising given the reprocessing of the line profile by the CGM and surrounding IGM. Including RXC J2248-ID3, there are now 11 $z > 6$ galaxies with Lyα profile and velocity offset measurements (see Figure 3(b)) where either [C II] 158 μm or [O III] 88 μm (Willott et al. 2015; Bradač et al. 2016; Inoue et al. 2016; Pentericci et al. 2016) or UV metal line detections (Stark et al. 2015a, 2017) constrain the systemic redshift. We discuss trends with M_{UV} and implications for the escape of Lyα from reionization-era galaxies in Section 4.

The WFC3/IR grism spectrum of RXC J2248-ID3 is shown along the bottom panel of Figure 2. Lyα is clearly detected, as was previously reported in Schmidt et al. (2016). The spectrum also reveals the detection of nebular C IV (unresolved) in both roll angles. The mean integrated flux ($(14.0 \pm 3.8) \times 10^{-18}$ erg cm^{-2} s^{-1}) and equivalent width (24.5 ± 7.1 Å) of the two roll angles thus reflects both C IVλ1548 and C IVλ1550. The grism spectra covers He II, O III], and C III], but no detections are apparent. The C IV to C III] flux ratio (>3.9 at 2σ) is slightly larger than the range (0.4–1.6) spanned by metal-poor C IV emitters at moderate redshifts (Stark et al. 2014; Vanzella et al. 2016) but is consistent with flux ratios expected for galaxies powered by low-

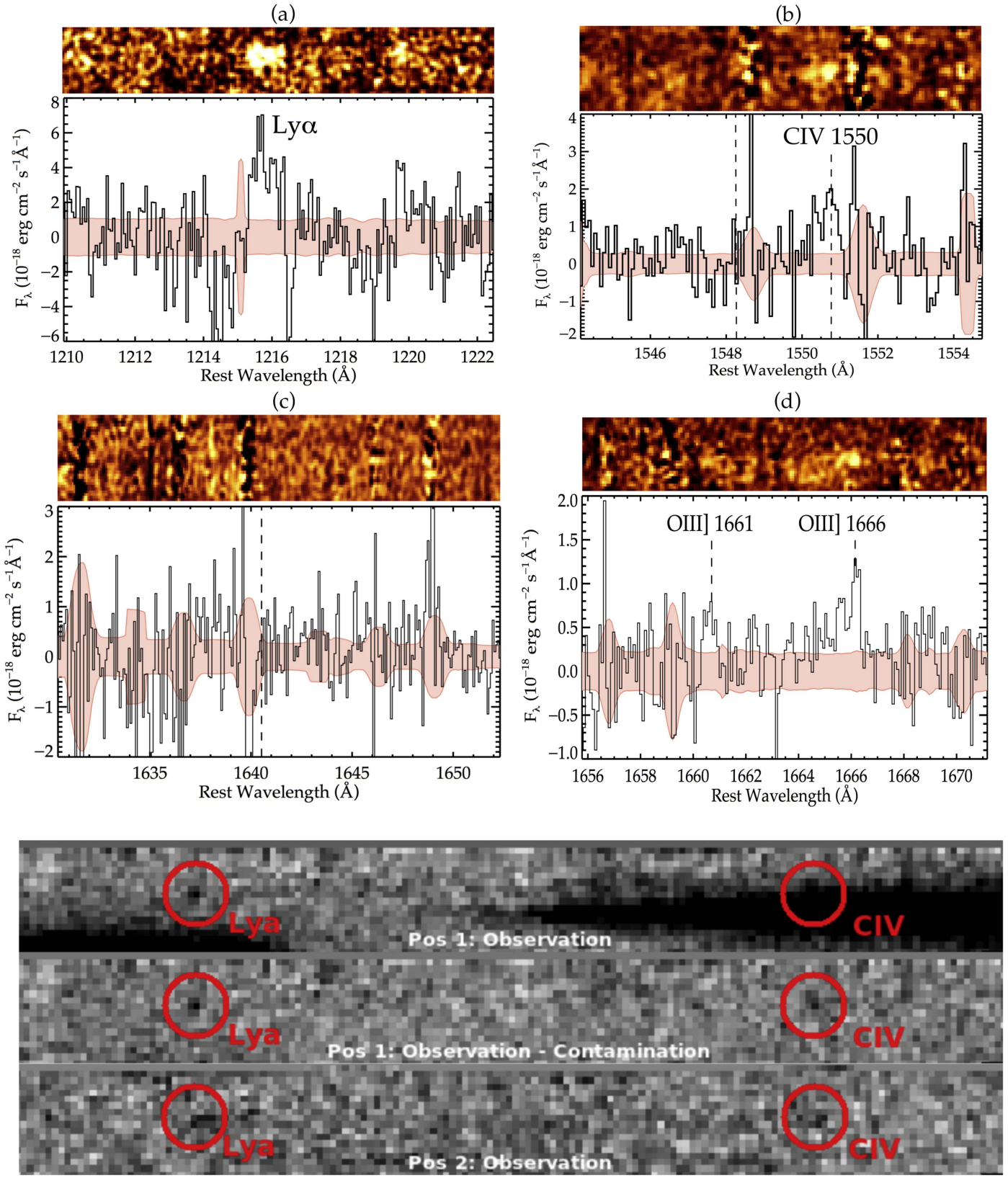

Figure 2. (Top) *Magellan*/FIRE spectrum ($R = 6000$) of the $z = 6.11$ galaxy RXC J2248-ID3. Each panel shows the 2D spectrum (with white corresponding to positive flux) on top of the 1D spectrum. The error in the 1D spectrum is shown in red. (Bottom) *HST* WFC3/IR G102 spectra ($R = 210$) of RXC J2248-ID3 at two different roll angles (black corresponds to positive flux), with the middle panel showing the spectrum following contamination subtraction.

metallicity stars (Feltre et al. 2016). The total C IV flux is consistent with the flux range ($(11.4–17.1) \times 10^{-18}$ erg cm^{-2} s^{-1}) predicted from the detection of the single C IVλ1550 component FIRE spectrum. Since the FIRE constraints on the O III], C IV, and He II fluxes are made under the same atmospheric conditions and are subject to the same aperture corrections, we will limit our

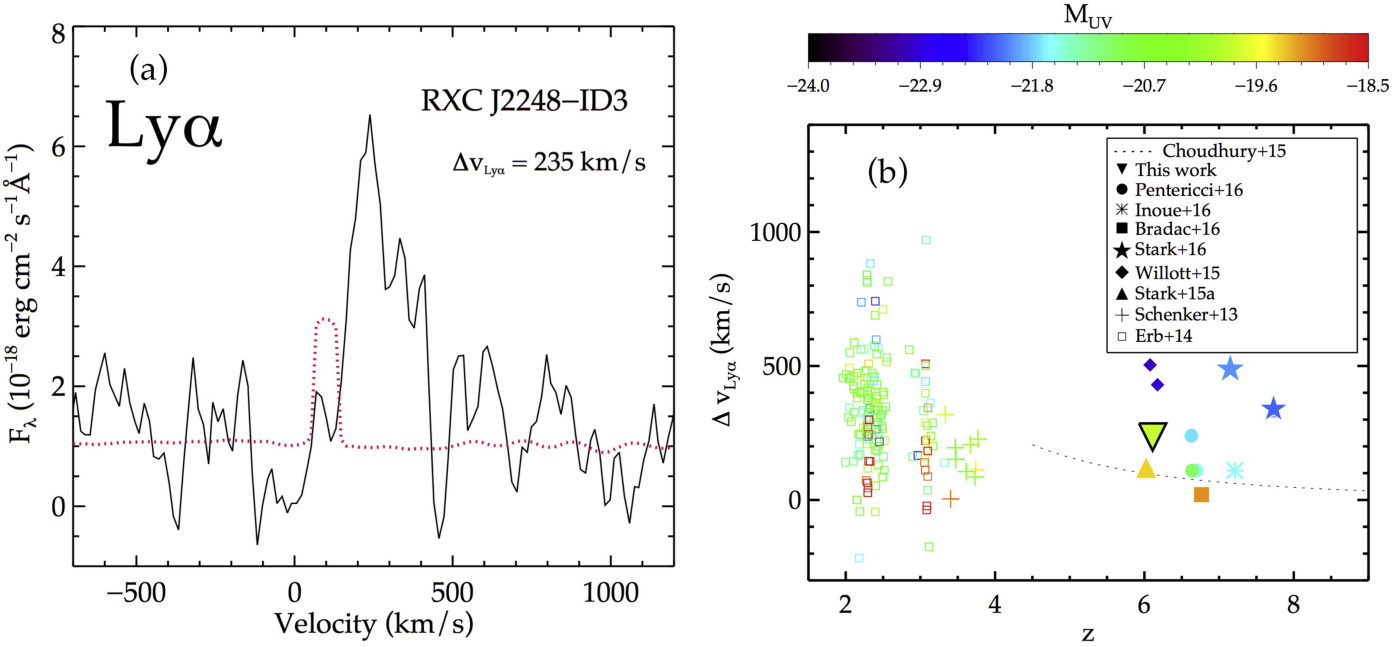

Figure 3. (Left) Lyα velocity profile of RXC J2248-ID3 derived using the systemic redshift from O III]λ1666. (Right) Lyα offset velocity ($\Delta v_{Ly\alpha}$) as a function of redshift. The dotted line represents velocity offset model used in Choudhury et al. (2015).

investigation to line ratios calculated from FIRE. In the empirically motivated case where C IVλ1548/C IVλ1550 = 1, we would expect log(He II/C IV) < -0.87 and log(O III]/C IV) $= -0.39$. The grism measurement places an upper bound on the total C IV flux (owing to slit losses), suggesting log(He II/C IV) < -0.96 and log(O III]/C IV) $= -0.51$. We will consider both options in the following section.

4. Discussion and Summary

The discovery of nebular C IV emission in RXC J2248-ID3 provides the second example of high ionization lines associated with an intrinsically faint lensed reionization-era galaxy. Yet the origin of the UV emission features remains poorly understood. The presence of multiple lines in the spectrum RXC J2248-ID3 provides a unique opportunity to examine the powering mechanism of the high ionization emission. Production of nebular C IV and O III] emission requires ionizing photons in the range 2.5–3.5 Ryd, but once in that state their multiplet emission is powered by collisional excitation at lower energies (~0.5 Ryd). As a pure recombination line, He IIλ1640 emission is powered by 4 Ryd ionizing photons. Photons with 4 Ryd are also capable of triply ionizing oxygen, thereby decreasing the strength of O III] emission.

The presence of strong O III] and C IV emission indicates that RXC J2248-ID3 must have an ionizing spectrum with significant power at 2.5–3.5 Ryd. But a rapid drop toward 4.0 Ryd is required to maintain strong O III] emission and explain the non-detection of an He II line. Such a spectral break is inconsistent with a shallow AGN power-law spectrum. The left panel of Figure 4 demonstrates this empirically. RXC J2248-ID3 and other metal-poor C IV emitters (Stark et al. 2014, 2015b; Berg et al. 2016; Vanzella et al. 2016) have larger O III]/C IV flux ratios than both $z \simeq 2$–3 UV-selected AGNs (Hainline et al. 2011) and the majority of type II $z \simeq 2$–4 quasars from Alexandroff et al. (2013). This follows naturally if the metal-poor galaxies have spectra that are deficient in the 4 Ryd photons that power He II and triply ionize oxygen.

The origin of the line emission can be clarified further by comparison to photoionization models. The right panel of Figure 4 shows the line ratios of RXC J2248-ID3 in the context of the AGN and stellar models from Feltre et al. (2016). RXC J2248-ID3 has log(O III]/He II) > 0.47, which is inconsistent with line ratios expected for AGNs (log(O III]/He II $= -3$ to -0.5), but can be easily explained by stellar models. In particular, a hard spectrum with a steep drop above 4 Ryd is characteristic of low-metallicity stellar populations. The precise metallicity required is dependent on the input stellar spectrum and may vary somewhat for single star models (like those considered in Feltre et al. 2016) and those that include binary evolution.

The presence of C IV in two of the first few $z > 6$ galaxies with deep spectra suggests that hard ionizing spectra may be more common in the reionization era. However, when considering whether the C IV emission in RXC J2248-ID3 is typical, it is important to remember that the galaxy was selected to probe the low-mass regime where metallicities may indeed be systematically lower. The existence of Lyα may further bias this selection toward low-metallicity (and low dust content) as well. Indeed, existing data at $z > 1.5$ suggest that nebular C IV emitters tend to be characterized by low stellar mass (2×10^6–1.1×10^8 $M_\odot$) and large equivalent width Lyα emission, as would be expected if the stellar populations capable of powering high ionization lines are only found among young, low-metallicity stellar populations. The nature of massive stellar populations at low metallicity remains poorly understood. Theoretical work on massive star binary evolution (e.g., Eldridge & Stanway 2009; de Mink et al. 2014) indicates that the lifetimes and high-energy ionizing output of massive stars at low metallicity may be vastly different (and higher) than classically assumed, potentially explaining the large luminosities now being detected in high ionization nebular lines.

Large samples of galaxies with intercombination metal line detections at high spectral resolutions can constrain $z > 6$ Lyα velocity offsets, a critical input for efforts to infer the IGM

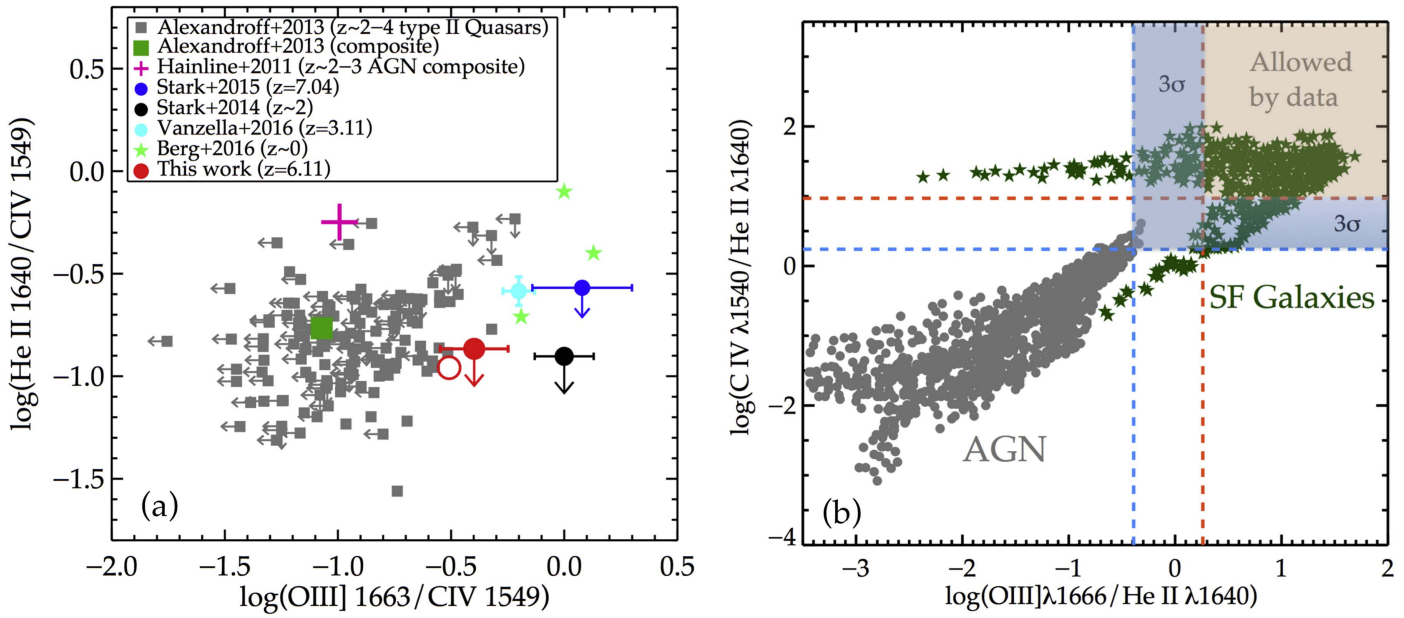

Figure 4. (Left) Comparison of UV line ratios associated with metal-poor C IV emitters and narrow-line AGNs at $z \sim 2$–4. The filled red circle shows the line ratios of RXC J2248-ID3 if we adopt the empirically motivated line ratio (C IVλ1548/C IVλ1550 = 1); the open red circle corresponds to an upper bound on the total C IV$\lambda\lambda$1548, 1550 flux adopted using the WFC3/IR grism measurement. The metal-poor star-forming systems are mostly separated from the AGN samples, suggesting they are subject to a softer radiation field. (Right) Comparison to photoionization models of Feltre et al. (2016). Gray (green) points correspond to flux ratios predicted from the AGN(stellar) photoionization models in Feltre et al. (2016). The red (blue) dashed line represents 1σ (3σ) lower limits on the line ratios, demonstrating that the data are better explained by a stellar radiation field.

ionization state from Lyα emitters. Our measurement of $\Delta v = 235\,\mathrm{km\,s^{-1}}$ in a sub-L* object ($M_{\rm UV} = -20.1$) at $z = 6.11$ falls between existing measurements of high-luminosity objects with large Lyα offsets and low-luminosity objects with small offsets at $z > 6$. In a partially neutral IGM, a large velocity offset will allow line radiation to redshift further into the damping wing by the time it encounters intergalactic hydrogen, thereby reducing IGM attenuation relative to systems with smaller offsets (Dijkstra & Wyithe 2010). This $M_{\rm UV}$–Δv relationship (Figure 3(b)) will thus help create a luminosity-dependent Lyα fraction, consistent with emerging measurements (Stark et al. 2017). This issue should be further clarified through increasing samples expected in the near future.

To summarize, the detections of C IV and O III] in a $z > 6$ galaxy possibly hint at a markedly different underlying stellar population in typical galaxies at $z > 6$ relative to those studied at lower redshift. The detection of high ionization UV features in RXC J2248-ID3 likely suggests that they are more common in the reionization era than previously expected. Taken together, this implies that extrapolations from lower redshifts may be missing a significant and qualitative change in the nature of photon production in the epoch of reionization.

We thank the anonymous referee for useful comments. D.P. S. acknowledges support from the National Science Foundation through the grant AST-1410155. We are grateful to Dawn Erb for providing Lyα velocity offset data from Erb et al. (2014).

References

Alexandroff, R., Strauss, M. A., Greene, J. E., et al. 2013, MNRAS, 435, 3306
Anders, P., & Fritze-v. Alvensleben, U. 2003, A&A, 401, 1063
Baldwin, J. A., Phillips, M. M., & Terlevich, R. 1981, PASP, 93, 5
Balestra, I., Vanzella, E., Rosati, P., et al. 2013, A&A, 559, L9
Berg, D. A., Skillman, E. D., Henry, R. B. C., Erb, D. K., & Carigi, L. 2016, ApJ, 827, 126
Boone, F., Clément, B., Richard, J., et al. 2013, A&A, 559, L1
Bradač, M., Garcia-Appadoo, D., Huang, K.-H., et al. 2016, ApJL, in press (arXiv:1610.02099)
Bruzual, G., & Charlot, S. 2003, MNRAS, 344, 1000
Caminha, G. B., Karman, W., Rosati, P., et al. 2016, A&A, 595, A100
Choudhury, T. R., Puchwein, E., Haehnelt, M. G., & Bolton, J. S. 2015, MNRAS, 452, 261
Christensen, L., Richard, J., Hjorth, J., et al. 2012, MNRAS, 427, 1953
Cowie, L. L., Hu, E. M., & Songaila, A. 2011, ApJL, 735, L38
de Mink, S. E., Sana, H., Langer, N., Izzard, R. G., & Schneider, F. R. N. 2014, ApJ, 782, 7
Dijkstra, M., & Wyithe, J. S. B. 2010, MNRAS, 408, 352
Eldridge, J. J., & Stanway, E. R. 2009, MNRAS, 400, 1019
Erb, D. K., Pettini, M., Shapley, A. E., et al. 2010, ApJ, 719, 1168
Erb, D. K., Steidel, C. C., Trainor, R. F., et al. 2014, ApJ, 795, 33
Feltre, A., Charlot, S., & Gutkin, J. 2016, MNRAS, 456, 3354
Hainline, K. N., Shapley, A. E., Greene, J. E., & Steidel, C. C. 2011, ApJ, 733, 31
Inoue, A. K., Tamura, Y., Matsuo, H., et al. 2016, Sci, 352, 1559
Kelson, D. D. 2003, PASP, 115, 688
Kümmel, M., Walsh, J. R., Pirzkal, N., Kuntschner, H., & Pasquali, A. 2009, PASP, 121, 59
Lotz, J., Mountain, M., Grogin, N. A., et al. 2014, BAAS, 223, 254.01
Monna, A., Seitz, S., Greisel, N., et al. 2014, MNRAS, 438, 1417
Oesch, P. A., van Dokkum, P. G., Illingworth, G. D., et al. 2015, ApJL, 804, L30
Pentericci, L., Carniani, S., Castellano, M., et al. 2016, ApJL, 829, L11
Postman, M., Coe, D., Benítez, N., et al. 2012, ApJS, 199, 25
Reddy, N. A., Steidel, C. C., Pettini, M., et al. 2008, ApJS, 175, 48
Robertson, B. E., Ellis, R. S., Dunlop, J. S., McLure, R. J., & Stark, D. P. 2010, Natur, 468, 49
Schmidt, K. B., Treu, T., Bradač, M., et al. 2016, ApJ, 818, 38
Schmidt, K. B., Treu, T., Brammer, G. B., et al. 2014, ApJL, 782, L36
Shapley, A. E., Steidel, C. C., Pettini, M., & Adelberger, K. L. 2003, ApJ, 588, 65
Simcoe, R. A., Burgasser, A. J., Schechter, P. L., et al. 2013, PASP, 125, 270
Stark, D. P. 2016, ARA&A, 54, 761
Stark, D. P., Ellis, R. S., Charlot, S., et al. 2017, MNRAS, 464, 469
Stark, D. P., Richard, J., Charlot, S., et al. 2015a, MNRAS, 450, 1846
Stark, D. P., Richard, J., Siana, B., et al. 2014, MNRAS, 445, 3200
Stark, D. P., Schenker, M. A., Ellis, R., et al. 2013, ApJ, 763, 129

Stark, D. P., Walth, G., Charlot, S., et al. 2015b, MNRAS, 454, 1393
Steidel, C. C., Erb, D. K., Shapley, A. E., et al. 2010, ApJ, 717, 289
Steidel, C. C., Hunt, M. P., Shapley, A. E., et al. 2002, ApJ, 576, 653
Tapken, C., Appenzeller, I., Noll, S., et al. 2007, A&A, 467, 63
Trainor, R. F., Strom, A. L., Steidel, C. C., & Rudie, G. C. 2016, ApJ, 832, 171
Treu, T., Schmidt, K. B., Brammer, G. B., et al. 2015, ApJ, 812, 114
Vanzella, E., De Barros, S., Cupani, G., et al. 2016, ApJL, 821, L27
Willott, C. J., Carilli, C. L., Wagg, J., & Wang, R. 2015, ApJ, 807, 180